

# Oriented Single-Crystal-like Molecular Arrangement of Optically Nonlinear 2-Methyl-4-nitroaniline in Electrospun Nanofibers

Dmitry V. Isakov,\* Etelvina de Matos Gomes, Luis G. Vieira, Tatsiana Dekola, Michael S. Belsley, and Bernardo G. Almeida

Centro de Física, Universidade do Minho, Campus de Gualtar, 4710-057 Braga, Portugal

**L**ow symmetry organic molecules are of special interest in materials engineering because the formation of anisotropic structures of organic crystals greatly expands the range of their potential applications. A special role is played by molecules with pronounced polar properties, which display a polar structural arrangement and may be used as multifunctional materials.<sup>1–4</sup>

Among this class of materials are those formed by benzene derivative push–pull chromophores, such as 4-nitroaniline (molecular dipole moment of 7.6 D), which exhibit extremely large molecular first order hyperpolarizability.<sup>5</sup> The large polarizability in such molecules originates from a donor–acceptor conjugated group linked through delocalized  $\pi$ -bonds facilitating an electronic charge transfer (CT) along the molecule. This feature is widely used in the design of new materials for applications such as optical data storage, telecommunications, and optical signal processing. A well-known nonlinear optical (NLO) material of this type is 2-methyl-4-nitroaniline ( $C_7H_8N_2O_2$ , hereafter MNA), a derivative of 4-nitroaniline in which a methyl  $CH_3$  group is substituted in the 2-position to achieve crystalline noncentrosymmetry. Crystals of MNA exhibit a very large phase matched second harmonic generation (SHG) with a figure of merit more than 2 orders of magnitude greater than that of lithium niobate.<sup>6</sup>

To design efficient NLO organic devices, it is very important to effectively control the molecular morphology and dipole orientation since the net effective dipole moment in polycrystalline materials with randomly oriented molecules can be very small

**ABSTRACT** In-plane aligned nanofibers of organic 2-methyl-4-nitroaniline (MNA) were produced by the electrospinning technique using a 1:1 weight ratio with poly(L-lactic acid). The fibers are capable of enormous efficient optical second harmonic generation as strong as pure MNA crystals in powder form. Structural, spectroscopic, and second harmonic generation polarimetry studies show that the MNA crystallizes within the fibers in an orientation in which the aromatic rings of MNA are predominantly orientated edge-on with respect to the plane of the fiber array and with their dipole moments aligned with the fiber axis. The results show that the electrospinning technique is an effective method to fabricate all-organic molecular functional devices based on polymer nanofibers with guest molecules possessing strong nonlinear optical and/or polar properties.

**KEYWORDS:** electrospinning · nonlinear optical materials · molecular orientation · nanofibers · functional systems

or even negligible. One widely used approach to obtain a macroscopic molecular orientation in polycrystalline NLO materials is the electric field poling of polymers doped with NLO chromophores. In this technique, the guest–host polymer is heated above its glass transition temperature and subsequently placed in a strong electric field before being allowed to cool. The initially disoriented NLO molecules align themselves along the applied electric field, and their orientation is locked-in by the polymer after cooling below the glass transition temperature.<sup>7–9</sup> One drawback of this method is that there is often a significant chromophore relaxation after the electric field is removed, which leads to a decrease of the anisotropic properties.

Another factor, limiting the application of this technique, is that practical concentrations of the NLO molecules are often limited to relatively low values due to chromophore–chromophore interactions.

Recently, it was shown that the electrospinning technique is a very powerful tool for controlling the morphology and

\*Address correspondence to dmitry@fisica.uminho.pt.

Received for review June 22, 2010 and accepted December 06, 2010.

Published online December 13, 2010. 10.1021/nn101413x

© 2011 American Chemical Society

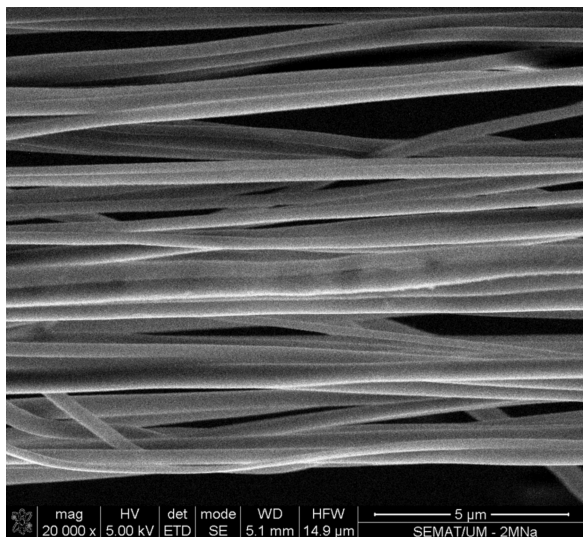


Figure 1. SEM image of MNA-PLLA nanofiber arrays.

molecular orientation of the polymer chains along electrospun fibers in different polymers and complexes.<sup>10–12</sup> Being a relatively simple and low-cost technique, electrospinning has been significantly developed in recent years. The method is based on the extrusion of a thin fiber from an electrically charged polymer solution provoked by an applied strong dc electric field.<sup>13</sup> Typically, the viscous polymer solution is loaded into a syringe with its needle connected to a high volt-

age source. At the threshold voltage, when the electrostatic forces overcome the surface tension of the polymer, the polymer droplet at the end of the needle is shaped into a Taylor cone and is continuously drawn into a fiber jet. The fibers are, in general, collected as a mesh on a grounded collector plate. The fiber diameter can vary from several nanometers up to several micrometers, depending on the parameters of the process, while their lengths can reach several meters.

The polymer chain orientation along the electrospun fiber is caused by shear stress and Coulombic forces acting synergistically on the polymer solution as the jet is accelerated by the electric field. This electrostatic molecular alignment provoked by the electrospinning process should be effective for all materials endowed with a large dipole moment, which suggests that the electrospinning technique can be used for producing fiber arrays with anisotropic polar properties.<sup>14</sup> In particular, it is an attractive technique for producing aligned organic materials with large hyperpolarizability since organic molecules can be easily incorporated into a polymer matrix.<sup>15</sup> Additionally, conventional electrospun nanofibers are continuous, which can be critical for optical waveguides based on NLO materials.

In this article, we demonstrate the implementation of this approach for producing a single-crystal-like oriented system with anisotropic nonlinear optical properties, based on aligned nanofibers of MNA obtained by the electrospinning technique.

## RESULTS AND DISCUSSION

**Structural Studies.** Fibers of MNA-PLLA were electrospun from 10% polymer solution with a 1:1 weight ratio of 2-methyl-4-nitroaniline (MNA) to poly(L-lactic acid) (PLLA). To produce thin aligned nanofiber arrays, a drum grounded collector rotated at 100 rpm was used. The obtained well-aligned MNA-PLLA fibers are uniformly shaped, slightly yellow tinged in color with an average diameter of 300 nm. As shown in Figure 1, the obtained fiber mat consists of a two-dimensional array of continuous nearly parallel nanofibers. Hereafter we will refer to the plane of the nanofiber array mat as the fiber plane.

Bulk crystals of MNA crystallize in the monoclinic  $I_a$  space group (a nonstandard setting of the  $Cc$  space group)<sup>16</sup> with  $a = 8.23 \text{ \AA}$ ,  $b = 11.62 \text{ \AA}$ ,  $c = 7.59 \text{ \AA}$ , and  $\beta = 94.1^\circ$ , with four molecules per unit cell. The molecule of MNA consists of an aromatic ring with the  $O_2N$  and  $NH_2$  groups in the para-position, while the methyl group occupies the ortho-position (Figure 2a). The molecular dipole moments of each molecule are nearly parallel to each other with the direction of the total dipole moment of the unit cell content lying in the (010) plane almost parallel to the  $X$  dielectric axis (the tilt angle is  $8^\circ$ ), as shown in Figure 2.

X-ray diffraction data indicate that the MNA molecules have crystallized within the electrospun fibers

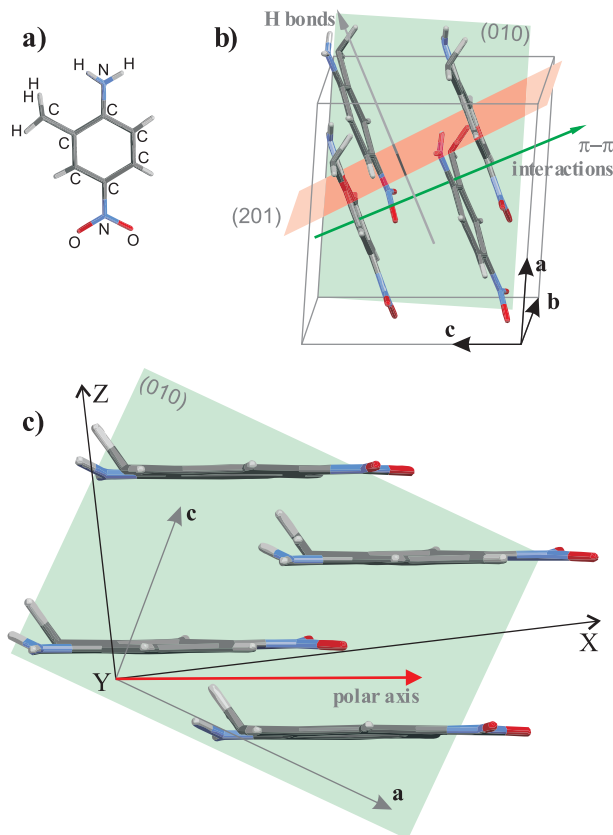


Figure 2. Molecule of MNA (a); MNA molecular packing (b) and its projection on the (010) plane (c).

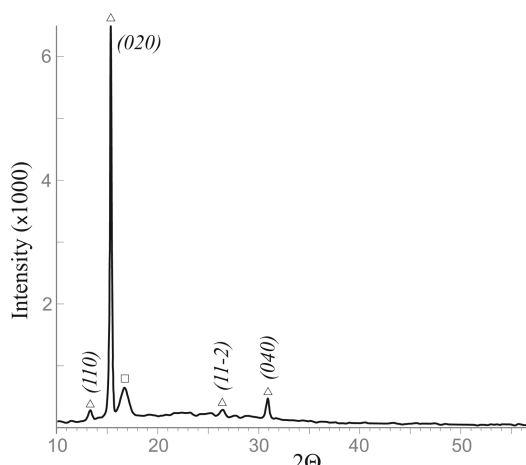


Figure 3. XRD pattern of MNA-PLLA fiber arrays ( $\triangle$  MNA,  $\square$  PLLA).

in a common orientation. By far, the most intense Bragg reflection observed in the measured diffraction pattern of the as-spun MNA-PLLA nanofibers corresponds to the (020) MNA reflection (Figure 3). The second most intense, although comparatively much weaker, reflection corresponds to the (040) MNA reflection. There are two other very weak reflections with a relative intensity ratio 1 order of magnitude smaller. A broader reflection at  $16.5^\circ$  corresponds to the characteristic semicrystalline PLLA diffraction peak.<sup>12</sup> These results indicate that MNA predominantly crystallizes inside the PLLA nanofibers with their (010) crystallographic plane parallel to the fiber array plane. Since the crystal structure of MNA belongs to the monoclinic point group *m*, the dielectric axes do not coincide with the crystallographic axes and vary with frequency. Here, as is usual with monoclinic point groups, we have chosen the dielectric *Y* axis to point along the two-fold crystallographic *b* axis, and the dielectric *X* and *Z* axis (hereafter, high frequency principal dielectric axis) as chosen by Lipscomb *et al.*<sup>17</sup> (Figure 2c). In this respect, one can conclude that the aromatic rings of the MNA molecules lie “edge-on” with

respect to the plane of the MNA-PLLA nanofiber arrays and the unit cell net dipole moment is approximately orientated within the plane of the fiber arrays.

FTIR spectroscopy was employed with the objective of determining the microscopic molecular orientation of MNA within the nanofibers. The polarized infrared spectra of MNA-PLLA nanofibers were obtained using two mutually perpendicular polarizations of the incident beam propagating normally to the fiber plane with the electric field vector oriented either along or perpendicular to the fibers’ alignment direction. As shown in Figure 4, quite different absorbance intensities were observed for the two polarizations. To avoid misinterpretation that might arise due to the superposition of MNA bands with those of the PLLA polymer, we consider only those peaks that do not coincide with any of the peaks in the spectrum of pure PLLA nanofibers. Consequently, only bands at 1632, 1602, 1580, 1508, 1480, 896, 825, 752, and 645  $\text{cm}^{-1}$ , which originate from the MNA crystal, will be examined. The assignments of these bands to the normal mode vibrations of the MNA molecule can be found in refs 18 and 20. Infrared absorbance measurements performed in single crystals<sup>18</sup> show that the set of bands (hereafter called set 1) at 1632  $\text{cm}^{-1}$  ( $\delta \text{NH}_2$ ), 1602  $\text{cm}^{-1}$  ( $\nu \text{CC}$ ), 1508  $\text{cm}^{-1}$  ( $\nu \text{NH}_2^{\text{as}}$ ), and 645  $\text{cm}^{-1}$  ( $\delta \text{CC}$ ) are more pronounced when light is polarized along the crystal polar axis (nearly parallel to the *X* axis), while the set of bands (hereafter called set 2) at 896  $\text{cm}^{-1}$  ( $\gamma \text{CH}$ ), 825  $\text{cm}^{-1}$  ( $\gamma \text{CH} + \gamma \text{C} - \text{NH}_2$ ), and 752  $\text{cm}^{-1}$  ( $\gamma \text{NO}_2$ ) are stronger for an incident polarization perpendicular to the polar axis.

Despite the polycrystalline character of MNA studied in the present work, we observe a strong dependence of the infrared spectra on polarization. Namely, bands of set 1 have higher intensities when the electric vector of the infrared beam is parallel to the fibers’ alignment axis. On the other hand, the three peaks of set 2 show higher intensity when light is polarized per-

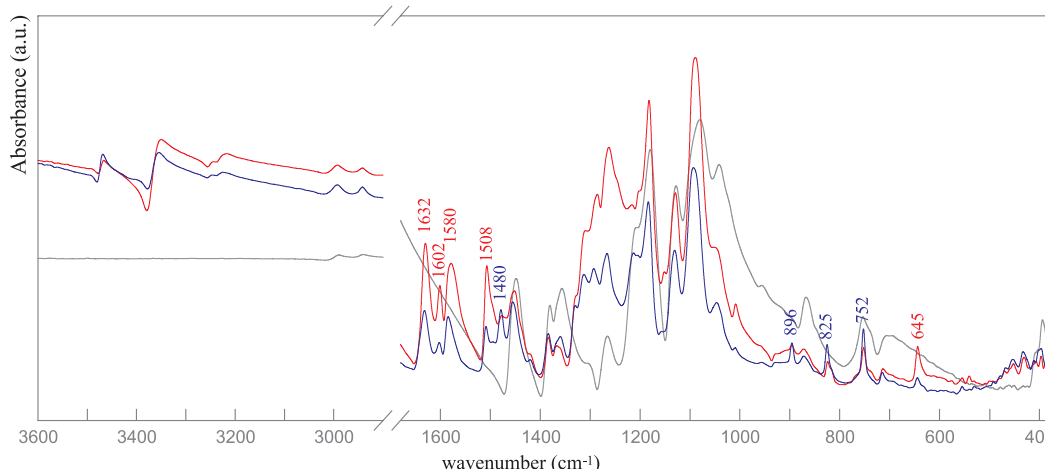


Figure 4. Polarized middle IR spectra of the aligned fibers oriented along (red curve) and perpendicular (blue one) to the polarization vector. The spectra of pure PLLA fibers (light gray) are shown for comparison.

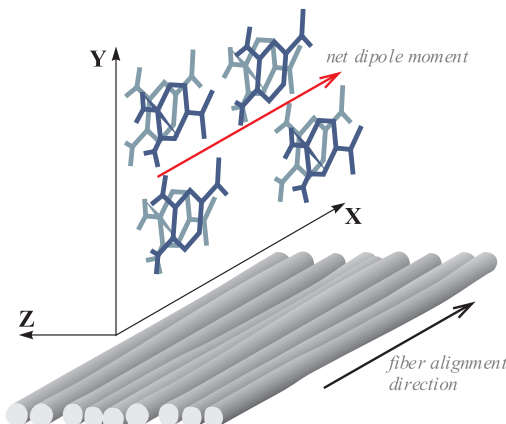


Figure 5. Schematic presentation of the aligned array of the electrospun fibers of MNA and their molecular orientation within the fibers' geometry. The X, Y, and Z axes are the principal dielectric axis of the MNA single crystal.

pendicularly to the fiber alignment axis. As pointed out by Okwieka *et al.*, the strong bands of set 2 originate from  $\pi-\pi$  interactions between neighboring molecules (see Figure 4). Notice that these interactions, which lie above and under the aromatic rings, are oriented along the Z direction (as shown in Figure 2b). Finally, the peak at  $1480\text{ cm}^{-1}$  ( $\nu\text{NO}_2 + \nu\text{CC}$ ), which shows up with a medium intensity for both polarizations in the single crystal spectra, is clearly present only when the incident polarization is perpendicular to the fiber's longitudinal axis.

Together, the X-ray diffraction pattern of MNA–PLLA fiber arrays and the observed polarized IR absorption spectra clearly indicate that the majority of the MNA crystals inside the MNA–PLLA nanofibers are oriented with their high frequency principal dielectric X axis aligned along the longitudinal axis of the nanofibers, while the aromatic rings are predominantly aligned perpendicular to the plane of the nanofiber mat. Figure 5 schematically shows the relative orienta-

tion of MNA molecules with respect to the aligned array of the electrospun MNA–PLLA nanofibers. Molecules of MNA are edge-on to the fiber array plane with the dielectric X axis lying along the fiber's longitudinal axes and the dielectric Z axis lying within the fiber array plane.

The observed orientation of the MNA dipole moment along the fiber axes is consistent with the premise that this dipole moment can easily be oriented by the strong electric field applied to the polymeric solution during the electrospinning.<sup>14,19</sup> Furthermore, this orientation is topologically favorable since, for rod-like molecules such as MNA, the bulk elastic energy is minimized when the long axis (that is, the crystal polar axis) of the molecules is parallel to the fiber axis.<sup>20</sup> It is less clear as to why, for different fibers, the MNA crystals tend to assume the same observed (010) planar orientation relative to the others. We speculate that the electrostatic forces, present during the fiber pulling process, acting on the high molecular polarizability lead to an asymmetric charge distribution on the fibers which in turn provokes a preferential orientation as they are collected on the grounded disk. Further work is needed to elucidate the detailed physical mechanisms responsible. However, regardless of the actual physical mechanisms involved, the MNA–PLLA nanofibers produced by the electrospinning method consisted of highly oriented MNA single-crystal-like structure incorporated into the polymer fiber host.

**Second Harmonics Generation Polarimetry.** To characterize the NLO properties of the obtained fibers, second harmonic generation polarimetry measurements were carried out. This is a unique tool for detection of degree of molecular assembly ordering.<sup>21</sup> To perform the measurements, an array of MNA–PLLA nanofibers mounted normally to the incident laser beam and the polarization angle  $\phi$  of the incident laser beam was varied. The generated second harmonic light was passed through an analyzer oriented either parallel ( $q-p$  configuration,

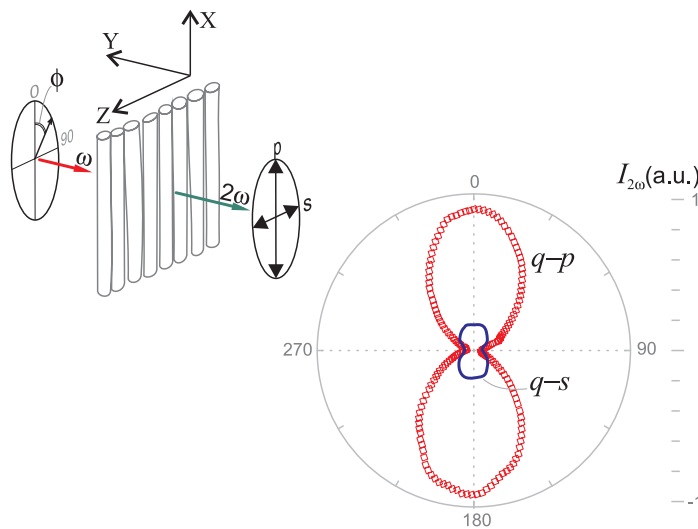


Figure 6. Sketch of the SGH ellipsometry experiment and SHG polarization patterns in the in-plane aligned array of the MNA–PLLA fibers.

( $q$  indicates an incident polarization angle) or perpendicular ( $q-s$  configuration) to the longitudinal axis of the aligned fibers, as shown on the Figure 6.

Given that MNA belongs to the space group  $I_a$  and keeping in mind the above established molecular orientation within the fibers, the SHG intensity  $I_{2\omega}$  generated by the MNA–PLLA nanofibers can be expected according to the following expressions:<sup>22</sup>

$$I_{2\omega}^{q-p} \propto [d_{11}\cos^2(\varphi) + d_{13}\sin^2(\varphi)]^2 I_{\omega}^2$$

and

$$I_{2\omega}^{q-s} \propto [2 \times d_{13}\cos(\varphi)\sin(\varphi)]^2 I_{\omega}^2$$

for  $q-p$  and  $q-s$  configurations, respectively. It should be noted that PLLA does not contribute any SGH signal.

These equations can be used to analyze the observed ellipsometry curves which satisfactorily fit the expected  $I_{2\omega}(\varphi)$  dependence. The  $d_{11}$  NLO coefficient dominates in MNA crystals ( $d_{11} > d_{13} \gg d_{16}, d_{21}, d_{22}$ ). From  $q-p$  and  $q-s$  curves, it is possible to estimate the ratio of  $d_{11}$  to  $d_{13}$ , which is around 4 and well consistent with the study in the MNA single crystal.<sup>23</sup> It should be noted that precise measurements of the effective NLO susceptibility coefficients in MNA fibers are complicated by the strong scattering from harmonic light from the  $d_{11}$  terms which can interfere with the second harmonic light originating from the other  $d_{ij}$  components of the matrix (in fact, the  $d_{11}$  scattering adds a significant background on the  $q-s$  curve).

To obtain an approximate value for the effective  $d_{11}$  coefficient of the MNA–PLLA nanofibers, we calibrated our experimental setup by carrying out a maker fringe measurement on a potassium dihydrogen phosphate (KDP) crystal. A (110) cut KDP crystal was used for which the appropriate second order coefficient is  $d_{36} = 0.39$  pm/V. Ignoring reflection losses, the peak of the envelope for the KDP maker fringes is given by

$$I_{2\omega}^{\text{KDP}} = A(d_{36}L)^2 I_{\omega}^2$$

where  $L$  is the KDP crystal thickness and  $A$  is a factor that takes into account the detection efficiency of our experimental setup. On the other hand, the  $q-p$  signal observed for  $\varphi = 0$  is given by

$$I_{2\omega}^{\text{fibers}} = A(d_{11}l)^2 I_{\omega}^2$$

where  $l$  is the effective thickness of the MNA crystals in the fiber mat. If we take as an upper limit for  $l$  the total

thickness of the fiber mat, we obtain as a minimum estimate for the effective nonlinear coefficient of the MNA–PLLA fibers  $d_{11} = 148 \pm 31$  pm/V.

Assuming the loss due to the light scattering through the polymer matrix, the obtained value of the  $d_{11}$  coefficient is in good agreement with  $d_{11} = 250$  pm/V measured by Levine *et al.*<sup>23</sup> Additionally, the effectiveness of NLO susceptibility of the randomly oriented MNA–PLLA nanofibers has been found to be as strong as the powder of MNA crystals with 100–120  $\mu\text{m}$  grain size measured by using Kurtz–Perry technique.<sup>24</sup>

## CONCLUSION

The study of well-aligned nanofibers of 2-methyl-4-nitroaniline produced from a PLLA solution by the electrospinning technique reveals a high degree of orientation of the MNA molecules along the fiber alignment axis. The relative molecular orientation of the MNA crystals within the obtained nanofibers has been confirmed by X-ray, FTIR, and the SHG polarimetry. The structural measurements revealed that the net transition dipole moment of MNA molecules is parallel to the longitudinal axis of the aligned nanofibers and that the  $\pi-\pi$  intermolecular interactions lie in the plane of the nanofiber arrays. That is, the molecules of MNA are predominantly oriented edge-on with respect to the plane of the fiber array. Uniaxially aligned MNA–PLLA nanofiber arrays show a strong polarization dependence of the second harmonic generation signal, further evidence that the molecular orientation assumes a nearly “single-crystal-like” structure. The second harmonic signal generated by a randomly oriented mat of MNA–PLLA fibers is as strong as that generated by a powder of MNA crystals with a grain size of 100–120  $\mu\text{m}$ . The NLO performance of the MNA–PLLA nanofiber arrays is as strong as those in bulk MNA, which makes such a system attractive for a variety of NLO applications.

Furthermore, the present study indicates that the electrospinning technique can be a powerful and efficient method for producing nanofibers with a high degree of guest molecular orientation within the polymer fiber host. This route for obtaining organic molecules with pronounced polar properties can be used for fabrication of functional nanofibers with quasi-crystalline structure and thus opens the way for the design of a wide class of all-organic devices.

## METHODS

The raw material of 2-methyl-4-nitroaniline and poly(L-lactic acid) (PLLA,  $M_w \sim 85\,000$ ), both purchased from Aldrich, were dissolved in chloroform/dimethylformamide in a 4:1 v/v ratio to contain 10 wt % of each compound. The obtained solution was stirred for several hours at ambient conditions prior to the electrospinning. Since MNA is not soluble in water, an appropriate solvent for

both the polymer and MNA should be found. Among several polymer choices (e.g., poly(ethylene oxide) or poly(vinyl alcohol)), PLLA was found to be the most appropriate because a PLLA/chloroform solution allows a 1:1 weight ratio of MNA and polymer precursors to be achieved. Additionally, the use of nonvolatile dimethylformamide permits us to effectively control the solution viscosity and consequently the diameter of the electrospun fibers.

The precursor solution was loaded into the syringe with its needle connected to the anode of a high voltage power supply (Spellmann CZE2000). To produce the in-plane aligned fiber arrays, 10–12 kV was applied to the needle when the grounded drum-rotating collector was rotating at 100 rpm. The distance between anode and collector was 12 cm, and precursor solution flow rate of 0.3 mL/h was controlled by a syringe pump. The alignment and fiber morphology were verified using a Leica Cambridge S360 scanning electron microscope at an accelerating voltage of 5–15 kV.

The electrospun MNA–PLLA fibers were studied by X-ray diffraction to characterize the MNA crystallization and crystallographic orientation in the fibers. The X-ray diffraction pattern of the aligned fibers was measured from classical  $\Theta$ – $2\Theta$  scans recorded on Bruker D8 Discover X-ray diffractometer using Cu K $\alpha$  radiation of wavelength 1.5406 Å between 10 and 60°. The lattice planes parallel to the substrate surface were determined from the  $q$  vector perpendicular to the fiber mat plane and correspondingly perpendicular to the longitudinal fiber axis (as the fiber mat is formed by an array of nearly parallel fibers).

Infrared absorption spectra were obtained using a Fourier transform infrared (FTIR) spectrometer (Bruker IFS 66 V) working in transmission mode in the frequency range of 380–7000 cm<sup>−1</sup> with 4 cm<sup>−1</sup> resolution. The polarized transmission spectra were recorded in vacuum using an incident beam light normal to the free-standing fiber mat with electric field either parallel or perpendicular to the fibers' alignment. We used a globar source, a KBr beam splitter, a KRS-5 polarizer and a DTGS:KBr detector.

The second harmonic generation response of the MNA–PLLA fibers was determined from transmission measurements through the fiber array, using a Q-switched Nd:YAG laser with 10 Hz, 20 ns pulses of 1064 nm light and the pulse energy of around 20 mJ. The fundamental beam passing through the sample was rejected by an appropriate filter, and an extremely bright SHG response was detected using an Hamamatsu photomultiplier tube, integrated with a boxcar (Standford Research 245).

To perform the SHG ellipsometry measurements, the aligned fiber arrays mounted on a glass plate were held by a goniometer stage in order to adjust the normal of the fiber mat to be along the direction of the incident laser beam. A half-wave plate (CVI part number QWPM-1064-05-2-R10) mounted in a stepper motor controlled rotation stage was used to rotate the polarization of the incident laser beam, while a Glan Taylor polarizer was used to analyze polarization of the second harmonic light generated by the fibers. The analyzer was fixed to be either parallel ( $q$ – $p$  configuration) or perpendicular ( $q$ – $s$  configuration) to the fibers' longitudinal axis (Figure 6). Care was taken to filter out the small amount of second harmonic light that can be generated by the quartz wave plate for certain angles before allowing the light to strike the fiber mat.

**Acknowledgment.** This work was financially supported by Fundação para a Ciéncia e Tecnologia (reference CIÉNCIA-2007 UMINHO-CF-06).

## REFERENCES AND NOTES

1. Horiuchi, S.; Kumaia, R.; Tokura, Y. Hydrogen-Bonded Donor–Acceptor Compounds for Organic Ferroelectric Materials. *Chem. Commun.* **2007**, 2321–2329.
2. Krebs, F. C.; Larsen, P. S.; Larsen, J.; Jacobsen, C. S.; Boutton, C.; Thorup, N. Synthesis, Structure, and Properties of 4,8,12-Trioxa-12c-phospho-4,8,12,12c-tetrahydrodibenzo[cd,mn]pyrene, a Molecular Pyroelectric. *J. Am. Chem. Soc.* **1997**, *119*, 1208–1216.
3. Zirkl, M.; Stadlobera, B.; Leisinga, G. Synthesis of Ferroelectric Poly(vinylidene fluoride) Copolymer Films and Their Application in Integrated Full Organic Pyroelectric Sensors. *Ferroelectrics* **2007**, *353*, 173–185.
4. Asaji, T.; Gotoh, K.; Watanabe, J. <sup>35</sup>Cl NQR of an Organic Ferroelectric Phenazine Chloranilic Acid Co-crystal. *J. Mol. Struct.* **2006**, *791*, 89–92.
5. Oudar, J. L.; Le Person, H. Second-Order Polarizabilities of Some Aromatic Molecules. *Opt. Commun.* **1975**, *15*, 258–262.
6. Chemla, D. S.; Zyss, J. In *Nonlinear Optical Properties of Organic Molecules and Crystals*; Academic Press: New York, 1987; Vols. 1 and 2.
7. Song, O. K.; Wang, C. H.; Guan, H. W. Effects of Electric Field Induced Dipolar Orientation on First- and Second-Order Optical Susceptibilities in Organic Guest/Host Systems. *J. Phys. Chem.* **1995**, *99*, 3540–3547.
8. Wright, M. E.; Mullick, S.; Lackritz, H. S.; Liu, L.-Y. Organic NLO Polymers. 2. A Study of Main-Chain and Guest–Host NLO Polymers: NLO-phore Structure *versus* Poling. *Macromolecules* **1994**, *27*, 3009–3015.
9. Jungbauer, D.; Teraoka, I.; Yoon, D. Y.; Reck, B.; Swalen, J. D.; Twieg, R.; Willson, C. G. Second-Order Nonlinear Optical Properties and Relaxation Characteristics of Poled Linear Epoxy Polymers with Tolane Chromophores. *J. Appl. Phys.* **1991**, *69*, 8011–8018.
10. Lee, K. H.; Kim, K.-W.; Pesapane, A.; Kim, H.-Y.; Rabolt, J. F. Polarized FT-IR Study of Macroscopically Oriented Electrospun Nylon-6 Nanofibers. *Macromolecules* **2008**, *41*, 1494–1498.
11. Kongkhlang, T.; Tashiro, K.; Kotaki, M.; Chirachanchai, S. Electrospinning as a New Technique To Control the Crystal Morphology and Molecular Orientation of Polyoxymethylene Nanofibers. *J. Am. Chem. Soc.* **2008**, *130*, 15460–15466.
12. Inai, R.; Kotaki, M.; Ramakrishna, S. Structure and Properties of Electrospun PLLA Single Nanofibres. *Nanotechnology* **2005**, *16*, 208–213.
13. Ramakrishna, S. In *An Introduction to Electrospinning and Nanofibers*; Fujihara, K., Teo, W.-E., Lim, T.-C., Ma, Z., Eds.; World Scientific Publishing Co.: Singapore, 2005.
14. Chang, C.; Tran, V. H.; Wang, J.; Fuh, Y.-K.; Lin, L. Direct-Write Piezoelectric Polymeric Nanogenerator with High Energy Conversion Efficiency. *Nano Lett.* **2010**, *10*, 726–731.
15. Isakov, D.; de Matos Gomes, E.; Belsley, M.; Almeida, B.; Martins, A.; Neves, N.; Reis, R. High Nonlinear Optical Anisotropy of Urea Nanofibers. *Europhys. Lett.* **2010**, *91*, 28007.
16. Hahn, T., Ed. *International Tables for Crystallography*; Springer: The Netherlands, 2002; Vol. A.
17. Lipscomb, G. F.; Garito, A. F.; Narang, R. S. Dispersion of the Nonlinear Second-Order Optical Susceptibility of an Organic System: *p*-Nitroaniline. *J. Chem. Phys.* **1981**, *75*, 1509–1516.
18. Okwielka, U.; Szostak, M. M.; Misiaszek, T.; Turowska-Tyrk, T.; Natkaniec, I.; Pavlukojć, A. Spectroscopic, Structural and Theoretical Studies of 2-Methyl-4-nitroaniline Crystal. Electronic Transitions in IR. *J. Raman Spectrosc.* **2008**, *39*, 849–862.
19. Kakade, M. V.; Givens, S.; Gardner, K.; Lee, K. H.; Bruce Chase, D.; Rabolt, J. F. Electric Field Induced Orientation of Polymer Chains in Macroscopically Aligned Electrospun Polymer Nanofibers. *J. Am. Chem. Soc.* **2007**, *129*, 2777–2782.
20. Vallée, R.; Damman, P.; Dosière, M.; Scalmani, G.; Brédas, J. L. A Joint Experimental and Theoretical Study of the Infrared Spectra of 2-Methyl-4-nitroaniline Crystals Oriented on Nanostructured Poly(tetrafluoroethylene) Substrates. *J. Phys. Chem. B* **2001**, *105*, 6064–6069.
21. Brasselet, S.; Zyss, J. Nonlinear Polarimetry of Molecular Crystals Down to the Nanoscale. *C. R. Phys.* **2001**, *8*, 165–179.
22. Sutherland, R. L. In *Handbook of Nonlinear Optics*; McLean, D. G., Kirkpatrick, S., Eds.; Marcel Dekker: New York, 2003.
23. Levine, B. F.; Bethea, C. G.; Thurmond, C. S.; Lynch, R. T.; Bernstein, J. L. An Organic Crystal with an Exceptionally Large Optical Second-Harmonic Coefficient: 2-Methyl-4-nitroaniline. *J. Appl. Phys.* **1979**, *50*, 2523–2527.
24. Kurtz, S. K.; Perry, T. T. A Powder Technique for the Evaluation of Nonlinear Optical Materials. *J. Appl. Phys.* **1968**, *39*, 3798–3813.